

Separation of spinal cord motor signals using the FastICA method

Yanmei Tie and Mesut Sahin

Department of Biomedical Engineering, Louisiana Tech University, 711 S. Vienna Street, Ruston, LA 71270, USA

E-mail: sahin@coes.latech.edu

Received 29 July 2005

Accepted for publication 12 August 2005

Published 30 September 2005

Online at stacks.iop.org/JNE/2/90

Abstract

Evoked motor signals descending down the corticospinal tract can be recorded selectively with multi-contact electrodes from the spinal cord surface. This method of extracting motor signals from the spinal cord may provide a means of communication for people with spinal cord injury. The information rate obtained with such an interface will improve if the separation of neural channels can be increased. In this study, the feasibility of increasing the channel separation was investigated using the blind source separation (BSS) technique. Neural signals recorded with multi-contact surface electrodes were treated as a linear mixture of independent neural sources located inside the spinal cord. Principal component analysis (PCA) was applied to estimate the dimensionality of the raw signals, and then the fixed-point FastICA algorithm was used to separate the primary neural sources from the secondary (smaller) ones. In all trials but one, the separation between the neural channels has increased by eliminating the secondary sources. These results suggest that the information rate of a spinal cord interface can be improved by separating the neural recordings into their independent components and selecting the ones with the largest distance between them. Comparison of independent component analysis (ICA) and PCA reveals that ICA performs better in this application.

(Some figures in this article are in colour only in the electronic version)

Introduction

Recordings of cortically evoked motor signals from the spinal cord surface with non-penetrating multi-contact electrodes have been investigated for spatial selectivity [1, 2]. The epidural or intradural recordings from the spinal cord during the stimulation of cortical points that were at least 1 mm apart suggested the presence of this selectivity. Although the spatial selectivity level, i.e., the channel separation, obtained in these preliminary tests was useful, it could benefit from further improvements for this method to be used as a multi-channel neural interface. Such a neural interface, which uses the corticospinal tract activity proximal to the point of injury, may serve as a spinal cord–computer interface (SCCI) for individuals with high-level spinal cord injury (SCI). The signals generated through this interface can then be used to substitute for the lost voluntary motor control.

The neural signals recorded with the multi-contact surface electrode were assumed to be a linear mixture of independent

neural sources inside the spinal cord in this study. Thus, the objective is to extract the source signals from a set of sensor measurements without any prior knowledge of the sources except for the assumption of independence. This paradigm is known as blind source separation (BSS) in signal processing theory [3]. The underlying principle in solving this problem is the independent component analysis (ICA) [4]. ICA is a statistical technique for transformation of multidimensional random vectors into components that are statistically as independent from each other as possible. ICA has received much attention in biomedical signal processing in recent years [5–10].

To solve the problem of ICA, Jutten and Herault first developed a fully recurrent feedback neural network and an unsupervised learning algorithm in 1991 [11]. Their algorithm was shown to work very efficiently with electroneurogram (ENG) signals contaminated by electromyogram (EMG) activity [10]. In 1995, Bell and Sejnowski proposed a

simple neural network algorithm, InfoMax, for carrying out ICA [12]. Since then, many investigators have explored new applications of ICA to biomedical signal processing, including electrocardiogram (ECG) [7], electroencephalogram (EEG) [6], event-related potentials (ERPs) [8] and functional magnetic resonance imaging (fMRI) [9].

In a preliminary study [13], an algorithm proposed by Cichocki and Unbehauen [14] was applied to the neural signals that were artificially mixed outside the spinal cord. This algorithm is a further improvement and extension of Jutten and Herault's method. It is robust and works efficiently even for badly scaled and ill-conditioned problems. Our results showed almost perfect separation of the two noiseless neural patterns that had an initial selectivity of less than 1%. Here, selectivity was defined as the average Euclidian distance between the vectors of the mixing matrix.

The neural activity used in this study was recorded with multi-contact electrodes from the spinal cord surface in anesthetized cats. The mixing of neural sources occurred naturally in the volume conductor of the spinal cord, and the projected signals were recorded from the surface. Therefore, the source signals were not accessible by the user. The fixed-point FastICA algorithm proposed by Hyvärinen [15] was applied to extract the independent neural sources from the surface recordings. The main objective of this study is to improve the channel separation of motor signals by eliminating the secondary (smaller) neural sources in the recordings using the FastICA method.

Methods

Data collection

The data used in this study were reported earlier [1, 2]. Briefly, the motor cortex around the cruciate sulcus was stimulated with tungsten microelectrodes in four adult cats under ketamine anesthesia. First, a pulse train (PW = 0.2 ms, $f = 330$ Hz, duration = 45 ms) was applied to the motor cortex to evoke muscle twitches in various parts of the contralateral forelimb (occasionally hindlimb) and thereby identify the corresponding areas of the motor cortex. A single pulse (PW = 0.2 ms, $I = 800 \mu\text{A}$) was then delivered to the motor cortex at a rate of 2 pulses s^{-1} to evoke a descending motor response in the lateral corticospinal tract (LCST) of the spinal cord. The cortical stimulation points were at least 1 mm apart to ensure that different groups of fibers were activated within the LCST. The evoked potentials were recorded from the cervical spinal cord surface using silicone substrate multi-contact (7 or 8 contacts) electrodes. The signals were acquired into a personal computer at a sampling rate of 80 000 samples s^{-1} using National Instruments Data Acquisition Board (PCI-6071E) and LabVIEW programming tool.

Data analysis

Seven trials were included in this study. Here 'trial' means a particular implantation of a multi-contact electrode on the spinal cord. Multiple trials were made in a given cat, and in each trial multiple recordings were obtained by stimulating

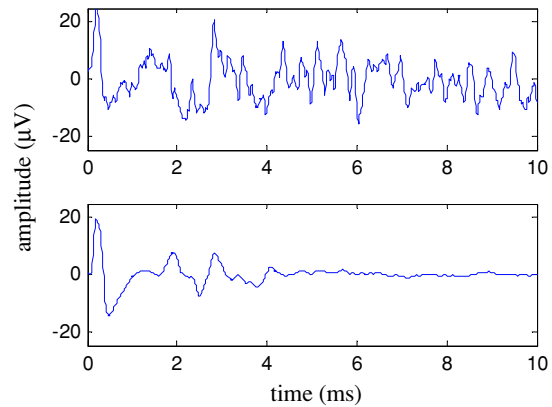


Figure 1. Extraction of the motor components from the spinal cord recordings using trigger-averaging method ($n = 256$). The top panel shows a single 10 ms long raw signal with contaminating neural components and background noise. The bottom panel shows the averaged version. The stimulus artifact appears within the first millisecond.

various cortical points. Each recording consisted of 256 acquisitions of 10 ms long neural signals during the repeated stimulation of the same cortical point.

Principal component analysis (PCA) was used to estimate the dimensionality of the neural sources inside the LCST. The results of PCA revealed that only one primary neural source predominated, i.e., the eigenvalues of other principal components were relatively much smaller (the eigenvalues of the second largest components were only $9.44 \pm 5.36\%$ of that of the predominant component). The secondary, smaller sources made the location of the primary neural sources more 'fuzzy' in the multidimensional space.

Each recording lasted 128 s (256 acquisitions obtained at a stimulus rate of 2 pulses s^{-1}). In order to test the temporal and spatial stability of the primary neural source during the stimulation of a single cortical point, the 256 acquisitions were divided into four equal segments. The 64 acquisitions of each segment were then trigger averaged to extract the motor component in the presence of a large background noise. Figure 1 shows a single acquisition of a raw signal and a trigger-averaged version with the stimulus artifact occurring within the first millisecond. The first millisecond of each acquisition was discarded to eliminate the stimulus artifact. Therefore, the averaged signal was 9 ms long and contained 720 data points at a sampling frequency of 80 kHz.

The envisioned paradigm for the locations of the independent neural sources inside the white matter is shown in figure 2. One primary neural source (large filled circle) and a few secondary sources (small circles) are depicted. These neural signals project to the spinal cord surface so that the recorded signal from each contact is a linear mixture of the projected signals from all the sources. The following linear mixture model describes the system:

$$\mathbf{x}(t) = \mathbf{A}\mathbf{s}(t), \quad (1)$$

where $\mathbf{x}(t)$ are the neural recordings from the multi-contact surface electrode and $\mathbf{s}(t)$ are the independent neural sources. \mathbf{A} is the unknown mixing matrix which depends on the volume

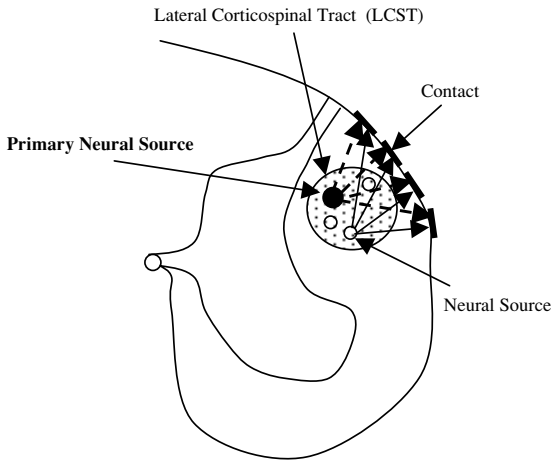


Figure 2. A depiction of the neural sources inside the lateral corticospinal tract (dotted area) and how they superimpose at the recording contacts. The large filled circle represents the primary neural source and others are the secondary neural sources. The recorded signal from each contact is a linear mixture of the projections from the sources.

conductor characteristics. The coefficients of A represent the relative projection strengths and polarities from the neural sources to the recording points (contacts) on the spinal cord surface.

The fixed-point FastICA algorithm was applied to separate the mixed signals into independent sources. Figure 3 is the block diagram of how the FastICA algorithm was performed to estimate the source signals. From 7 or 8 contacts in each recording, a reduced set of 4-contacts was centered by subtracting the sample mean and used for analysis. Then, the trigger-averaged signals were fed into the FastICA algorithm to be separated. At the output of the algorithm, the estimated independent sources $\hat{s}(t)$ are shown as

$$\hat{s}(t) = Wx(t), \quad (2)$$

where W is the de-mixing matrix. Derived from equations (1)

and (2), W is the inverse of the mixing matrix A , i.e.,

$$W = A^{-1}. \quad (3)$$

Out of 89 recordings, 64 (71.91%) reached convergence in all of the four segments. These data were included in the study.

Each output channel represented an estimated neural source. The correlation operation between the estimated sources ($\hat{s}(t)$) and the mixed signals ($x(t)$) was performed to determine the primary neural source. The estimated source ($\hat{s}_i(t)$) that had the largest sum of the correlation coefficients (absolute value) with the mixed signals was considered as the primary source because it had the largest contribution to the mixture.

During the 128 s stimulation process, the sources were assumed to move slowly within the white matter, indicated by the slight variations in the mixing matrix A across the four segments of each recording. To test if the primary neural source was relocating within the cord as a function of stimulation point in the cortex, and not so much within a recording, the multivariate analysis of variation (MANOVA) was performed. In the MANOVA test, the peak-to-peak measurements of the first volley of the neural activity in the mixed signals and the reconstructed primary sources were used. The recordings in each trial were then clustered into groups of two, three or four. Those recordings that had the largest distances between their primary sources were grouped together. The α values of MANOVA before and after FastICA were compared to see if the channel separation was improved by selecting the primary neural source and eliminating the secondary sources. The MANOVA test was also performed on the results of PCA for comparison.

Results

The trigger-averaged version of the recordings overlaid by the projected signals from the neural sources is shown in figure 4. Each projection is calculated by scaling the estimated independent source with the corresponding column of the

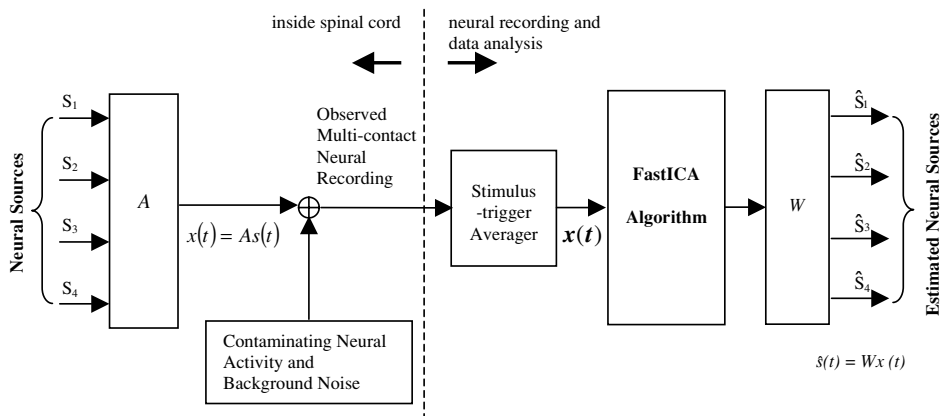


Figure 3. A block diagram of how the FastICA algorithm was applied to obtain the estimated sources from the multi-contact recordings. The observed multi-contact recording, $x(t)$, is a linear mixture of the sources, $s(t)$. Matrix A contains the weighting coefficients. The trigger-averaged signals are fed into the FastICA algorithm to be separated. After convergence of the FastICA algorithm, the de-mixing matrix W is obtained. The output consists of four estimated source signals.

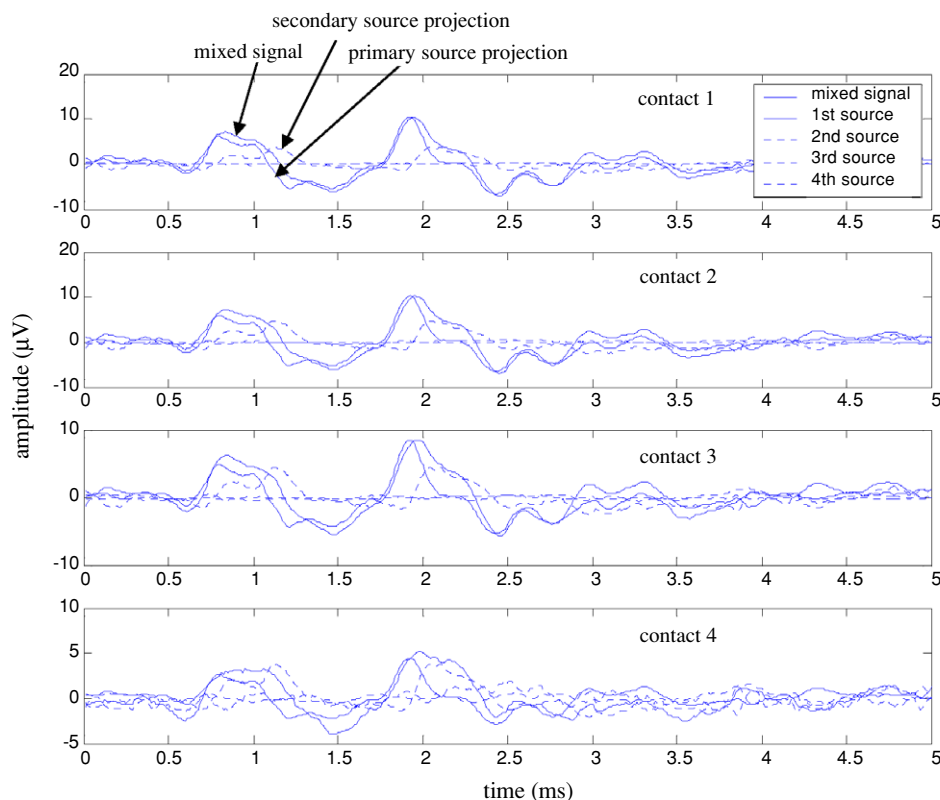


Figure 4. An example of the averaged version of the 4-contact recording overlaid by the projections from the four sources. Each projection is calculated by scaling the estimated independent source with the corresponding element of the mixing matrix \mathbf{A} . Among four reconstructed sources, one stands out having the largest correlation coefficients with the mixture. This source is the primary neural source, which is the first one in this example.

Table 1. Correlation coefficients between the mixed signals and the reconstructed projections of the four estimated sources for each contact. The correlation measure between the mixture and the projections from the estimated signals was performed to identify the primary neural source. The results of the example data shown in figure 4 indicated that the first source had the largest correlation coefficient with the mixture (shown in bold numbers).

Mixed Signals of	Projections from the estimated sources			
	#1 (Primary)	#2	#3	#4
Contact #1	0.9866	0.0060	0.1588	0.0382
Contact #2	0.9601	0.0240	0.2736	0.0521
Contact #3	0.9340	0.0278	0.3485	0.0739
Contact #4	0.6417	0.5730	0.5098	0.0042

mixing matrix \mathbf{A} . Table 1 shows the correlation coefficients between the mixture and the four contributing sources into each contact. The reconstructed projection from the first source stands out having the largest correlation coefficients with the mixture. This is the primary neural source. The variation analysis showed that the primary sources contained $74.51 \pm 10.43\%$ of the total energy of the mixed signals across all the data in this study. Due to the ambiguity of the order in which the output channels of the FastICA algorithm are arranged [16, 17], the dominant (primary) source could occur in any output channel.

The column of \mathbf{A} that corresponded to the projection from the primary neural source was called the ‘primary source column’. Figure 5 shows the plot of the ‘primary source column’ for three different recordings in a trial. For

each recording, the mean and the standard deviation of the coefficients across the four segments are plotted. The fact that the mean projection strengths vary between recordings indicates that the source is relocating in the spinal cord as the stimulation point in the cortex is moving. In order to find out if this relocation is significant compared to the random walking of the source during the stimulation of one cortical point, the analysis of variance was applied. The recordings were clustered into two, three or four subgroups based on the results of MANOVA test as described in methods. The subgroups were chosen to minimize the α value, which maximize the separation between the recordings (neural channels). Alpha values of the MANOVA test are listed in table 2 for original signals (mixed), after ICA and after PCA. It can be concluded from these α values that in a trial there were at least a

Table 2. Alpha values of the MANOVA test. Data from seven trials in four cats were included in this study. A varying number of recordings converged in each trial during the application of the FastICA algorithm. The recordings were clustered into two, three or four subgroups based on the results of the MANOVA test. The recordings in each subgroup had the smallest α value, indicating the largest separation of the signals. Compared with the original signals, the α values decrease as a result of the FastICA method (except for the first trial, shown as bold numbers), indicating improvement of the channel separation. In most trials (shown in italic bold numbers), the PCA did not provide further separation of the signals.

Trial no.	Cat no.	No. of converging recordings	No. of subgroups	α of MANOVA test		
				Original signal	After ICA	After PCA
1	1	3 of 9	2	0.0047	0.0339	0.0737
			3	0.1595	0.8214	0.0737
2	1	6 of 8	2	0.0587	0.0005	0.0421
			3	0.1357	0.0278	0.2293
			4	0.1638	0.1164	0.2293
3	1	3 of 3	2	0.2060	0.0243	0.4067
			3	0.4252	0.1134	0.5351
4	1	9 of 9	2	0.0015	0.0001	0.0180
			3	0.0241	0.0017	0.0964
			4	0.1478	0.0056	0.0426
5	2	5 of 13	2	0.4795	0.0028	0.0934
			3	0.4795	0.0421	0.4948
			4	0.5247	0.4099	0.9258
6	3	22 of 26	2	0.2342	0.0001	0.0221
			3	0.2590	0.0010	0.2693
			4	0.3388	0.0098	0.9787
7	4	16 of 21	2	0.2845	0.0001	0.1432
			3	0.3931	0.0012	0.5879
			4	0.4266	0.0021	0.5879

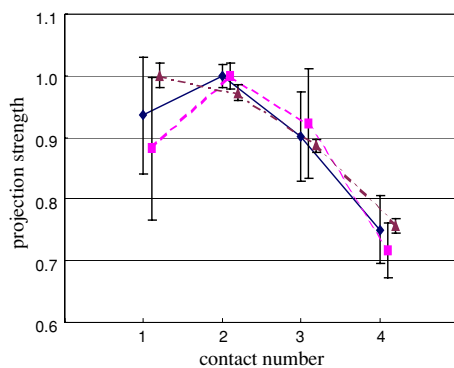


Figure 5. A plot of the ‘primary source column’ of mixing matrix A of three different recordings of an example trial. For each recording, the mean and the standard deviation of the ‘primary source column’ of A across the four segments are plotted. The Y-axis represents the projection strength of the primary source to the contact. The contact number is indicated by the X-axis. The standard deviation bars indicate how much variation takes place across the four segments during a 128 s recording. The α value of the MANOVA test was 0.8392 for the mixture and 0.7491 after ICA process. Each plot is shifted slightly in horizontal direction for the clarity of the figure.

few spatially separated primary neural sources during the stimulation of different points in the motor cortex. Compared with the original signals, the α value decreased in all cases as a result of the FastICA algorithm (except for the first trial, shown in bold numbers), indicating that the channel separation was

improved when the secondary sources were eliminated from the mixed signals.

The α values after the ICA were always smaller than those following the PCA, except for one case (second line in the table). In most cases (shown in italic bold numbers), the PCA did not improve the channel separation of the original signal.

Conclusions

The results of this analysis support the conclusions of the previous work [1] that the cortical stimulation points can be distinguished using multi-contact recordings of the descending signals from the spinal cord surface. This suggests that a multi-channel spinal cord–computer interface may be feasible.

In this study, we applied the FastICA algorithm in order to improve the channel separation of spinal cord surface recordings. The channel separation was improved in all cases except one by the FastICA technique. Comparison of ICA and PCA revealed that ICA is more suitable for this application.

Discussion

In a preliminary study, we demonstrated a successful separation of artificially mixed real neural signals using the Cichocki and Unbehauen algorithm [13]. As an extension, we tested the algorithm with a larger number of channels and used percent crosstalk as a measure of separation. The results

showed that perfect separation could be achieved when the parameters of the learning rule, such as the initial learning rate and the exponential coefficient of the decreasing learning rate in the convergence phase, were chosen properly.

In this study, the fixed-point FastICA algorithm was applied to improve the channel separation of spinal cord surface recordings. There were 7 or 8 contacts (channels) in each recording and different numbers of contacts were tested for the best separation. Some of the contacts were excluded from analysis because of a large stimulation artifact or excessive noise in the recording. A trade-off existed between the convergence speed of the FastICA algorithm and the number of input channels. Multiple trials indicated that decreasing the number of channels made the algorithm easier to converge. Four was chosen as the number of input channels to include the maximum amount of data in the analysis while having a stable convergence.

Unlike in the adaptive learning algorithms, the computations of the FastICA algorithm were made in batch mode, i.e., a certain number of data points were used in a single step (720 data points in this study). The convergence is slow with the adaptive learning algorithms, whereas the fixed-point iteration algorithm has very fast and reliable convergence. Although the FastICA is non-adaptive, it has advantages of neural algorithms, i.e. it is parallel, distributed, computationally simple and requires little memory space [15]. The stochastic gradient methods are more suitable for a fast changing environment, while the fixed-point algorithm's appealing convergence properties make it a very good choice in an environment where fast real-time adaptation is not necessary. We used the fixed-point FastICA algorithm assuming that the neural source locations in the cord will be reproducible for the same cortical points, thus the \mathbf{A} matrix will be constant over time.

Unlike the preliminary study [13], where the recordings were artificially mixed by taking the weighted sum of multiple neural patterns, naturally mixed multi-contact recordings were used in this study. The mixing of neural sources occurred in the volume conductor of the spinal cord while the projections were recorded from the surface (figure 2). Therefore, we do not have access to the neural sources, which makes it difficult to validate the assumptions made about the sources for carrying out ICA. This problem is very common in the application of ICA method on biomedical signals. Some of these assumptions were tested as follows.

First, since the assumption of the mutual independence of the unknown neural sources cannot be tested, the correlation coefficients between each pair of the estimated sources were calculated. The results were nearly zero, indicating mutual uncorrelatedness of the estimated sources. In contrast, the correlation coefficients between each pair of the mixed signals were large (0.8686 ± 0.0554).

Second, another important assumption about the sources, the probability distribution function, was considered. Normal plot and K-S test tools were applied to test the non-Gaussianity of the estimated sources. The results showed that in each recording, the primary source had non-Gaussian distribution. The other three sources were always non-Gaussian distributed,

with rare cases where one source appeared close to Gaussian (K-S test could not reject the null hypothesis at $\alpha = 0.05$). However, the ICA still converged when only one of the independent components was Gaussian [18]. The mixed signals were tested as non-Gaussian distributed as well. Furthermore, the kurtosis measurements of the mixed signals and the estimated sources were compared since maximizing the non-Gaussianity is one of the characteristic outcomes of ICA when the signals are separated successfully. The results showed that the absolute values of the kurtosis of the mixed signals were always smaller than those of the estimated sources, indicating that the mixed signals were more Gaussian than the estimated sources.

PCA is a classical statistical method which has been widely used in data analysis and compression. The main difference between PCA and ICA is that PCA only uses the second-order statistics, while ICA imposes independence on higher order statistics [3]. Therefore, PCA only ensures that the output channels are *uncorrelated*, while ICA ensures that the output signals are *independent*. In our case, the ICA takes advantage of the randomness introduced into the signals by variations in the nervous system, which makes the sources more independent of each other. The results of this study demonstrate that the FastICA algorithm is effective in increasing the channel separation of spinal cord recordings, while PCA does not improve the channel separation. The BSS technique has also shown to be effective in improving the channel separation for the whole nerve recordings of the peripheral nerves [10].

Acknowledgment

Supported by a Biomedical Engineering Grant from The Whitaker Foundation (RG-01-0366).

References

- [1] Sahin M 2001 Selective recordings of motor signals from the corticospinal tract *Proc. Int. Functional Electrical Stimulation Society (Cleveland, Ohio, USA)*
- [2] Sahin M 2004 Information capacity of the corticospinal tract recordings as a neural interface *Ann. Biomed. Eng.* **32** 823–30
- [3] Haykin S (ed) 2000 *Unsupervised Adaptive Filtering: Volume 1. Blind Source Separation* (New York: Wiley)
- [4] Comon P 1994 Independent component analysis: a new concept? *Signal Process.* **36** 287–314
- [5] Liang H 2001 Adaptive independent component analysis of multichannel electrogastrogram *Med. Eng. Phys.* **23** 91–7
- [6] Jung T-P, Humphries C, Lee T-W, Makeig S, McKeown M J, Iragui V and Sejnowski T J 1998 Extended ICA removes artifacts from electroencephalographic recordings *Adv. Neural Inform. Process. Syst.* **10** 894–900
- [7] Jung T-P, Makeig S, Lee T-W, McKeown M J, Brown G, Bell A J and Sejnowski T J 2002 Independent component analysis of biomedical signals *The 2nd Int. Workshop on Independent Component Analysis and Signal Separation* pp 633–44
- [8] Makeig S, Westerfield M, Jung T-P, Covington J, Townsend J, Sejnowski T J and Courchesne E 1999 Functionally independent components of the late positive event-related

- potential during visual spatial attention *J. Neurosci.* **19** 2665–80
- [9] McKeown M J, Jung T-P, Makeig S, Brown G, Kindermann S S, Lee T-W and Sejnowski T J 1998 Spatially independent activity patterns in functional magnetic resonance imaging data during the stroop color-naming task *Proc. Natl Acad. Sci. USA* **95** 803–10
- [10] Winter J, Rahal M, Taylor J and Donaldson N 1999 Blind separation of EMG and ENG cuff electrode recordings *Proc. 1999 IEEE Eng. in Med. and Bio. 21st Ann. Conf. and the 1999 Fall Meeting of the Biom. Eng. Soc. (1st Joint BMES / EMBS) (Atlanta, Georgia, USA)* p 581
- [11] Jutten C and Herault J 1991 Blind separation of sources: Part I. An adaptive algorithm based on neuromimetic architecture *Signal Process.* **24** 1–10
- [12] Bell A J and Sejnowski T J 1995 An information maximization approach to blind separation and blind deconvolution *Neural Comput.* **7** 1129–1159
- [13] Tie Y and Sahin M 2002 Separation of multi-channel spinal cord recordings using unsupervised adaptive filtering *Proc. 2nd Joint EMBS/BMES Conf. (Houston, Texas, USA)* pp 2014–5
- [14] Cichocki A and Unbehauen R 1996 Robust neural networks with on-line learning for blind identification and blind separation of sources *IEEE Tran. Circuits Syst. I* **43** 894–906
- [15] Hyvärinen A 1999 Fast and robust fixed-point algorithms for independent component analysis *IEEE Tran. Neural Netw.* **10** 626–34
- [16] Cichocki A and Unbehauen R 1993 *Neural Network for Optimization and Signal Processing* (New York: Wiley)
- [17] Tong L, Liu R-W, Soon V C and Huang Y-F 1991 Indeterminacy and identifiability of blind identification *IEEE Trans. Circuits Syst.* **38** 499–509
- [18] Hyvärinen A and Oja E 2000 Independent component analysis: algorithms and applications *Neural Netw.* **13** 411–30